Wind and Structures, Vol. 1, No. 4 (1998) 351-364
DOI: http://dx.doi.org/10.12989/was.1998.1.4.351

Wind tunnel blockage effects on aerodynamic behavior of bluff body

Chang-Koon Choi†

Department of Civil Engineering, Korea Advanced Institute of Science and Technology(KAIST), 373-1 Kusong-dong, Taejon 305-701, Korea

Dae-Kun Kwon‡

Department of Civil Engineering, KAIST, Korea

Abstract. In wind tunnel experiments, the blockage effect is a very important factor which affects the test results significantly. A number of investigations into this problem, especially on the blockage correction of drag coefficient, have been carried out in the past. However, only a limited number of works have been reported on the wind tunnel blockage effect on wind-induced vibration although it is considered to be fairly important. This paper discusses the aerodynamic characteristics of the square model and square model with corner cut based on a series of the wind tunnel tests with various blockage ratios and angles of attack. From the test results, the aerodynamic behaviors of square models with up to 10% blockage ratio are almost the same and square models with up to 10% blockage ratio can be tested as a group which behaves similarly.

Key words: blockage effect; wind-induced vibration; wind tunnel experiment.

1. Introduction

The wind-induced problems of civil/architectural structures are divided into two main categories. One is the static problem due to the static or static equivalent wind loads, and the other is the wind-induced vibration problem. The general wind-resistant design of structures should be performed with careful considerations of the wind effects on the structures. The construction of large structures such as long span bridges and tall buildings, which are relatively light and flexible structures, is recently on the increase. However, these structures tend to have low levels of intrinsic damping and can be especially prone to the high resonance when subjected to wind. For this reason, many structural engineers take more interest in wind lately. To understand and clarify the aerodynamic characteristics of the structural systems due to wind, the wind tunnel test is dominantly used as a powerful investigative tool and the trend will continue in the foreseeable future although the fields of theoretical and computational fluid

† Institute Chair Professor
‡ Graduate Student

mechanics are being developed rapidly.

In the wind tunnel experiments, the design of sophisticated test model is very important and will be determined by applying the similarity with the real structure. However, the geometric scale of test model is severely limited by the blockage effect of wind tunnel. While the real structures are exposed to the infinite space (natural state), the experimental test is performed in the limited space (wind tunnel) having boundary layer. For avoiding the excessive distortion of the flow due to this effect, many design codes limit the allowable blockage ratios which are generally no greater than 5% even though some codes allow a little more ratio, for example 10% (ASCE Standard 1997, Honshu-Shikoku Bridge Authority 1980, The Bridge and Wind 1990, Japanese Architectural Center 1994, Houghton and Carruthers 1976, Liu 1991). The ratio is defined as projected areas of the test model on a plane normal to the test-section axis (blockage area) over the sectional size of wind tunnel.

Many investigations on this problem associated with the limited blockage ratio, especially on the blockage correction of drag coefficient (C_D), have been carried out. Maskell (1963) was the first who examined this effect, and proposed the blockage correction method of C_D as the 2nd order equation using the blockage factor. Cowdray (1967), Sykes (1973) and Awbi (1978) extended Maskell's theory to rectangular sections. Laneville *et al.* (1986) suggested the correction equation being applicable to the cross section of reattachment type. Takeda *et al.* (1992) examined the applicability of the Maskell's theory to the various kinds of sections and to the wind-induced vibration. Noda *et al.* (1993) considered this effect in the turbulent flow. As the majority of studies on the blockage effect is in the drag coefficients, the rules of blockage ratio in the design codes have been determined mainly based on these results of C_D correction studies. Only a limited number of investigations concerning the wind tunnel blockage effect on wind-induced vibration have been made in the past even though the construction of wind-sensitive structures is recently on the sharp increase (Takeda and Kato 1992).

As mentioned above, the ratio of the test model to the real structure is determined by blockage ratio to avoid the undesirable blockage effect in the test. As the slight modification of the shape of model may induce a big difference in the aerodynamic characteristics, especially in the wind-induced vibration, manufacturing the detailed exact test model is also the important factor to be considered when the blockage ratio is determined. The larger blockage ratio is allowed, the more realistic aerodynamic behavior of the structure is expected to be obtained. When the real structure is complex, or the size of test model is not sufficient to describe the exact shape of real structure to include the necessary details, the problem can be solved either by increasing the scale of test model or by building a large wind tunnel test facilities. The latter approach will be simpler but cost a lot. Therefore, as an alternative, the former approach is adopted in this study. However, to increase the scale of test model, the code limit manufactured in accordance with the use of increased blockage ratio must also be allowed.

This study focuses on the investigations into the possibility and effects of using increased blockage ratio beyond the code limit in the wind tunnel test. In addition, the aerodynamic behaviors of the selected test model (B/D=1.0) are evaluated and the correlation between the aerodynamic behaviors, the galloping and vortex-induced vibration with the various blockage ratios and angles of attack is parametrically examined. Finally, the conclusion on the possible use of increased blockage ratios in the wind tunnel test is drawn.

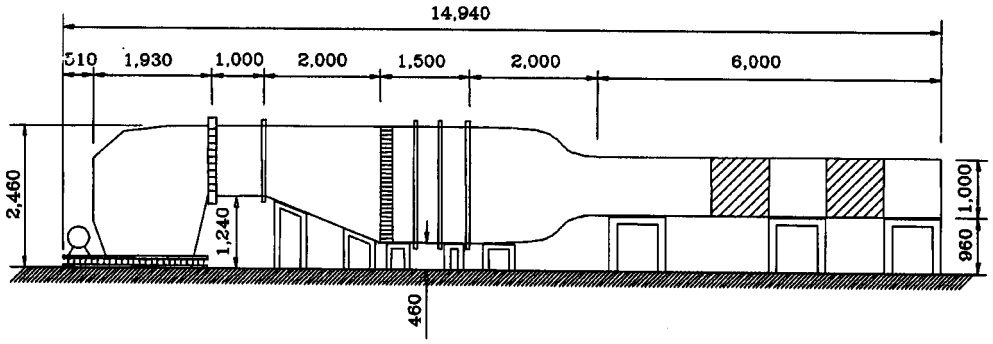

Fig. 1 Wind tunnel at KAIST Civil Engineering

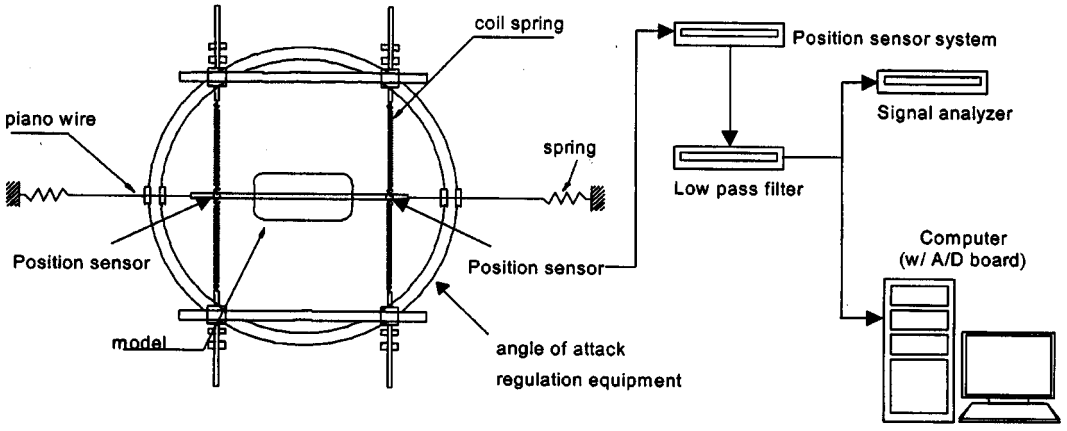

Fig. 2 Set-up of the model and measurement systems

2. Experimental Procedure

2.1. Experimental equipment

The experiments were carried out on the Eiffel type (open-circuit type) wind tunnel at Korea Advanced Institute of Science and Technology (KAIST) whose test section is 1 m × 1 m and the length of test zone is 4 m (Fig. 1). The wind velocity is controlled by the fan speed (RPM), and maximum velocity is about 17.0 m/s, measured by the Pitot tube and digital manometer.

To measure the dynamic response (displacement) caused by the galloping and vortex-induced vibration, the sectional model test is carried out in the smooth flow. The test model was set up to have two response modes; namely, the across-wind mode and the torsional mode. The movement of the test model in the flow direction is restrained. Through the pre-testing, it has been known that wind-induced vibration occurs only in the across-wind mode but does not occur in the torsional mode (Fig. 2).

2.2. Test model and conditions

The change of test section in wind tunnel without changes of the test model to obtain the

desired blockage ratios in the test is profitable as it easily sets the same test condition, but the flow in the wind tunnel may not be uniform, and may be more expensive. Therefore, the approach of manufacturing the models in accordance with the blockage ratios is adopted in this study.

The wind tunnel experiment is performed first to measure the aerodynamic response of two-dimensional square section cylinder (B/D=1.0) in the smooth flow. And then, the square models with corner cut were tested. Considering the wind tunnel size, tests are carried out with the seven different blockage ratios (S/C), i.e., 3, 5, 7.5, 10, 12.5, 15 and 20%. The size of corner cut is uniformly 1/10D in all cases (Fig. 3) (Choi and Kwon 1999).

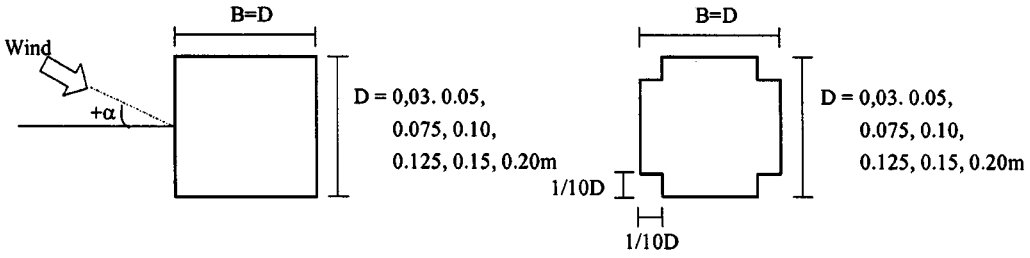

(a) square model (b) square model w/ corner cut

Fig. 3 Cross-sectional shapes of test model

Table 1 Wind tunnel test conditions

(a) square model

Blockage ratio (S/C)	Mass/unit length(kg/m)	Across-wind frequency(Hz)	Logarithmic damping ratio(δ)	Mass-damping parameter $\frac{m\delta}{\rho D^2}$
3%	1.05	5.344	0.015	14.523
5%	1.17	4.938	0.012	4.661
7.5%	1.65	4.532	0.010	2.434
10%	1.98	4.281	0.009	1.479
12.5%	2.77	3.656	0.008	1.177
15%	3.21	3.438	0.007	0.829
20%	4.04	2.969	0.005	0.419

(b) square model with corner cut

Blockage ratio (S/C)	Mass/unit length(kg/m)	Across-wind frequency(Hz)	Logarithmic damping ratio(δ)	Mass-damping parameter $\frac{m\delta}{\rho D^2}$
3%	1.1	5.344	0.017	17.243
5%	1.25	4.938	0.015	6.244
7.5%	1.72	4.532	0.014	3.553
10%	2.11	4.281	0.012	2.101
12.5%	2.95	3.656	0.01	1.567
15%	3.37	3.438	0.009	1.119
20%	4.14	2.969	0.007	0.601

The aerodynamic responses are measured under various angles of attack, from 0° to 45° increasing 5 degrees a step and by increasing the wind velocity 0.2 m/s a step. The positive direction of attack angle is defined that the upwind side of the model lifts (Fig. 3). Test conditions are given in Table 1.

3. Results of square model

3.1. Aerodynamic characteristics of square model

The two important aerodynamic phenomena of this square model to be investigated are the galloping and the vortex-induced vibration (VIV). As the galloping is the oscillation of divergent

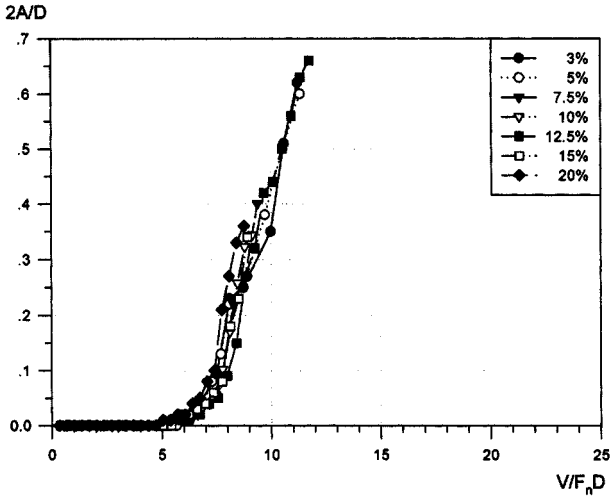

Fig. 4 The aerodynamic behaviors for the square model (α=0°)

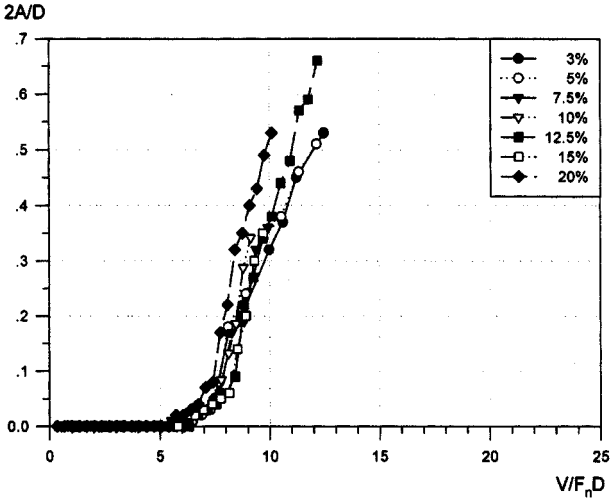

Fig. 5 The aerodynamic behaviors for the square model (α=5°)

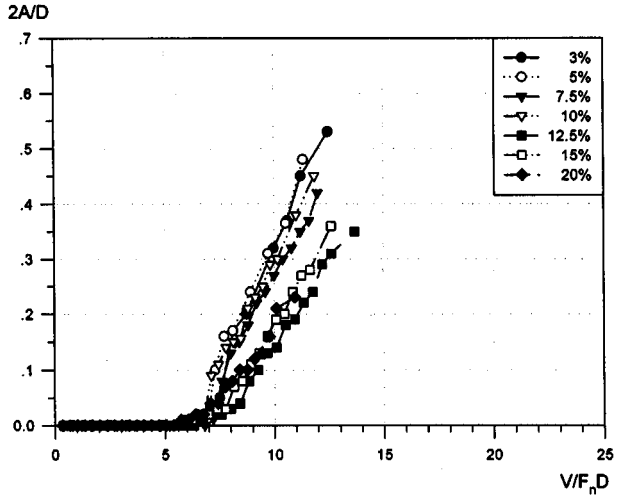

Fig. 6 The aerodynamic behaviors for the square model (α=10°)

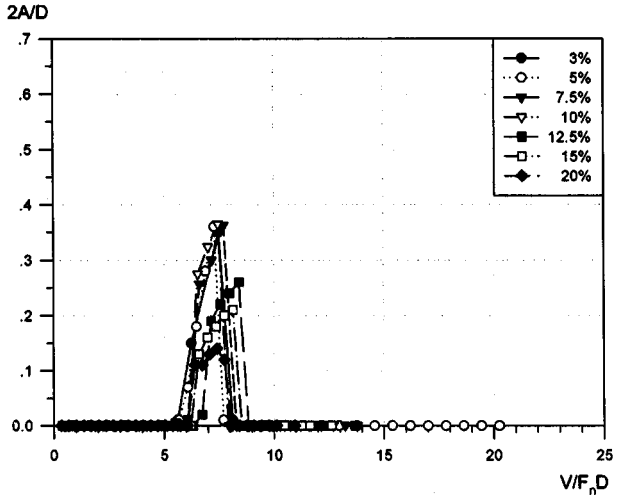

Fig. 7 The aerodynamic behaviors for the square model (α=15°)

type, this phenomenon must be checked at the onset velocity. The VIV is the limited oscillation, which occurs within a certain range of wind velocity only and leads gradually to the problems of structural fatigue and of serviceability. There are four checkpoints in the VIV, i.e., the onset velocity, extinction velocity, the maximum response, and the velocity of the maximum response. To find out the maximum allowable blockage ratio, a parametric study based on the above mentioned five factors, i.e., one for the galloping and four for the VIV, is carried out.

For the easy evaluation and comparison, all the test values are converted into the non-dimensional values. In the Figs. 4~21, the horizontal axis (x-axis) are scaled to the reduced velocity (V_r=V/F$_n$D) and the vertical axis (y-axis) are scaled to the non-dimensional response (2A/D).

Figs. 4~13 show the test results of square model. While the galloping phenomenon occurs when the angle of attack(α) is smaller than 10°, VIV with somewhat large amplitudes occurs when α is

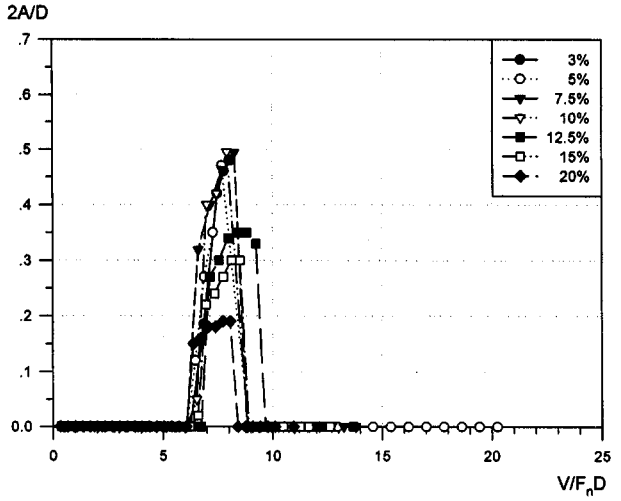

Fig. 8 The aerodynamic behaviors for the square model (α=20°)

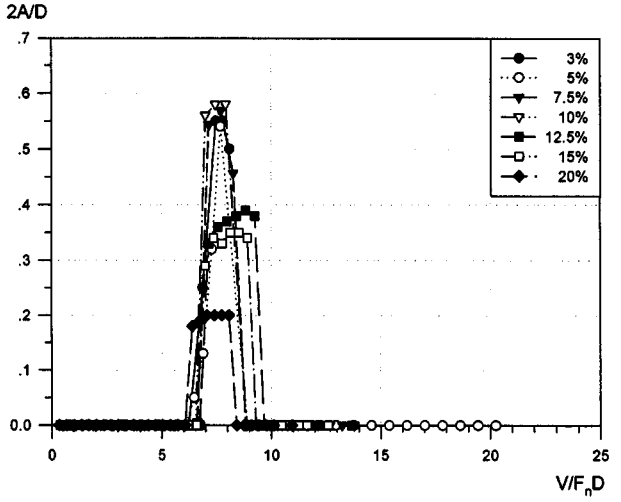

Fig. 9 The aerodynamic behaviors for the square model (α=25°)

larger than 15°, that is the known critical occurrence point of the galloping phenomenon.

3.1. Blockage effect for the galloping phenomenon

As shown in Figs. 4, 5, 6 (α=0°, 5°, 10°, respectively), the onset reduced velocity of the galloping of the models are almost same for all the blockage ratios considered in this study. The slightly different responses or amplitudes are shown for different blockage ratios. It is also observed that as the attack angle increases, the discrepancy of responses tends to increase and the larger blockage ratio shows the smaller responses. However, the discrepancy is not significant in the view that the onset velocity is more important than aerodynamic responses on the galloping phenomenon, the galloping phenomenon show the similar aerodynamic

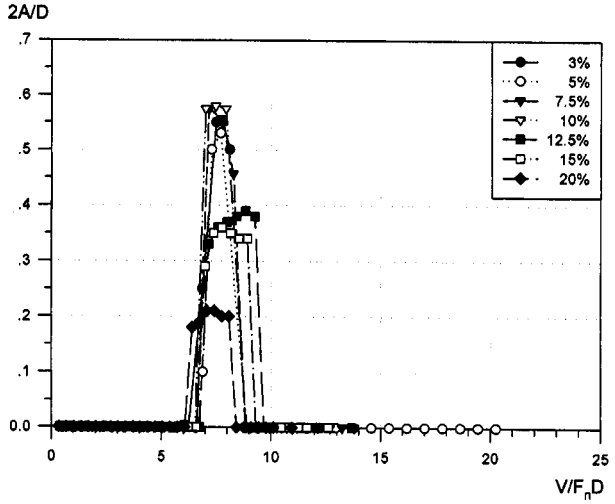

Fig. 10 The aerodynamic behaviors for the square model (α=30°)

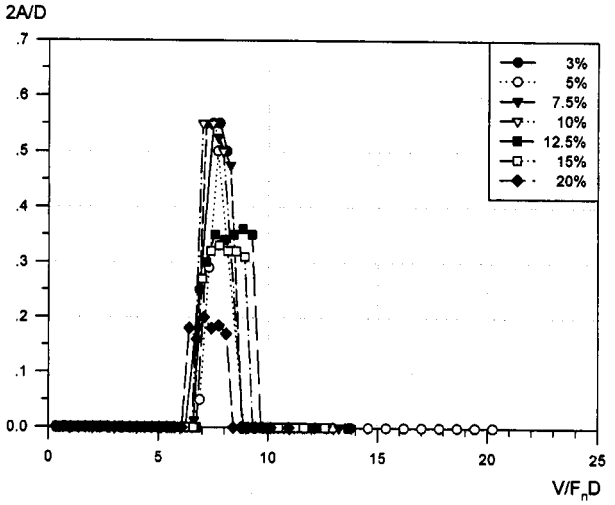

Fig. 11 The aerodynamic behaviors for the square model (α=35°)

behaviors regardless of the blockage ratios.

3.2. Blockage effect for the vortex-induced vibration

As the angle of attack is increased to 15°, the vortex-induced vibration phenomenon appears. Figs. 7~13 show the results of vortex-induced vibration for α=15°~45°. Since the test model in this study has a relatively small dimensional ratio (B/D), the appearance of Karman type VIV only is observed. The flow separates at the upwind corners and advances by cyclically alternating vortices that form by turns at the top and bottom edges, and are swept downstream.

The onset and extinction reduced velocities of models with up to 10% S/C, i.e., $V_r \cong 6.5$, 9.0, respectively, show good agreements and the maximum response occurs at nearly same V_r

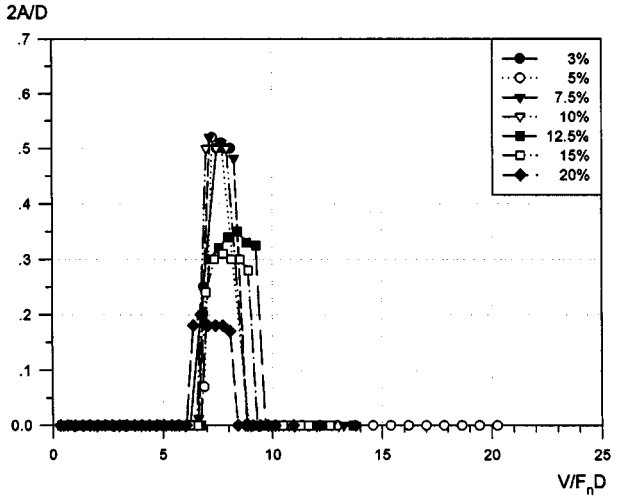

Fig. 12 The aerodynamic behaviors for the square model (α=40°)

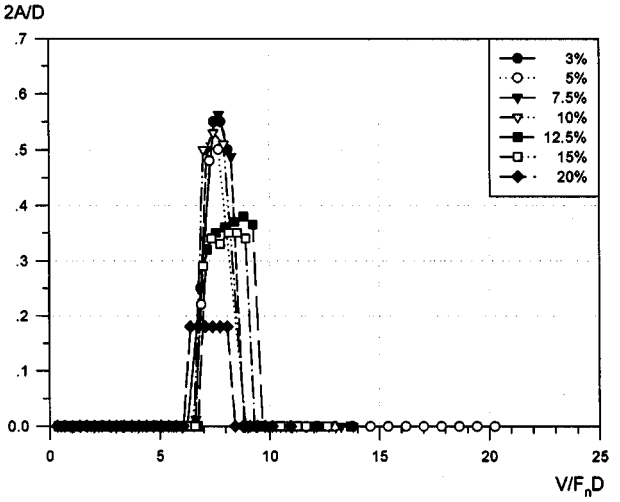

Fig. 13 The aerodynamic behaviors for the square model (α=45°)

($V_r \cong 7.0$). However, in case of models with over 10% S/C, the onset, extinction velocities and the velocity of the maximum response become quite different.

To compare the maximum responses of different the blockage ratios, using the value of 5% blockage ratio as a basis, values (displacements) of 3% is scaled up, and those of 7.5, 10, 12.5, 15 and 20% are scaled down in proportion to the depth(D). As shown in Figs. 7~13 in case of models with up to 10% S/C, the maximum responses are nearly the same while in cases of models with over 10% S/C. There are large discrepancies in the maximum responses for the different blockage ratios. Therefore, it has been tentatively concluded that the aerodynamic behaviors for vortex-induced vibration of models with up to 10% S/C can be clearly distinguished from those of models with over 10% S/C and the former can be separately treated as a group which behaves almost identically.

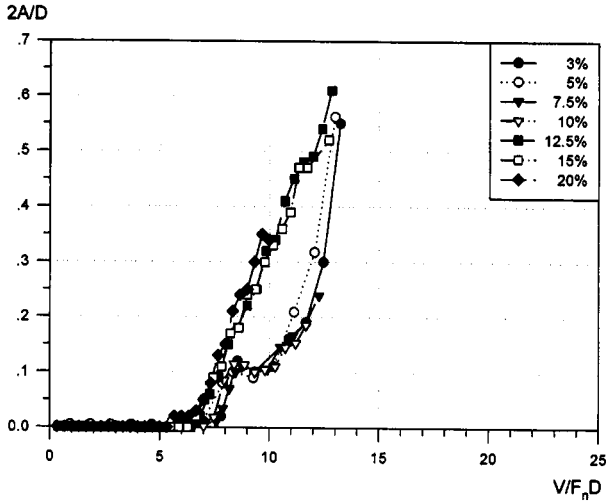

Fig. 14 The aerodynamic behaviors for the square model with corner cut (α=0°)

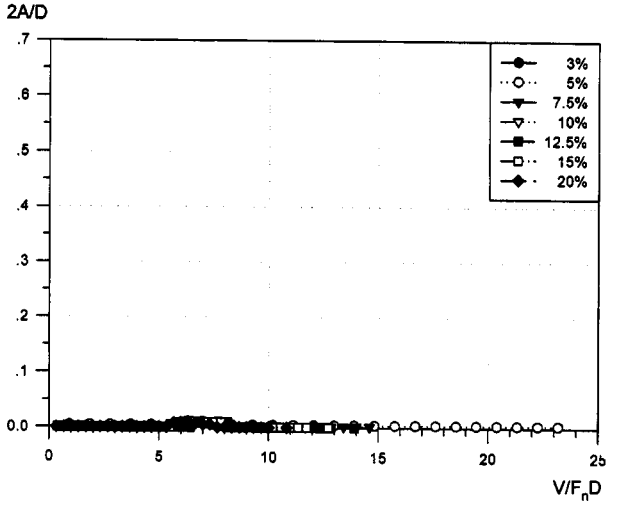

Fig. 15 The aerodynamic behaviors for the square model with corner cut (α=15°)

4. Results of square model with corner cut

4.1. Aerodynamic characteristics of square model with corner cut

To verify what has been found out about the aerodynamic behaviors of square models of different S/C in the previous model, the square models with corner cut were tested. Corner cut has been known to be a kind of aerodynamic improvement technique which is very efficient to suppress the galloping phenomenon in the rectangular sections with relatively small dimensional ratios (B/D) such as bridge towers and tall buildings. Therefore, the galloping occurs only at α=0°, no occurrence at any other angles including α=5, 10° due to the effect of aerodynamic improvements by the corner cut. When α is larger than 20°, the vortex-induced vibration

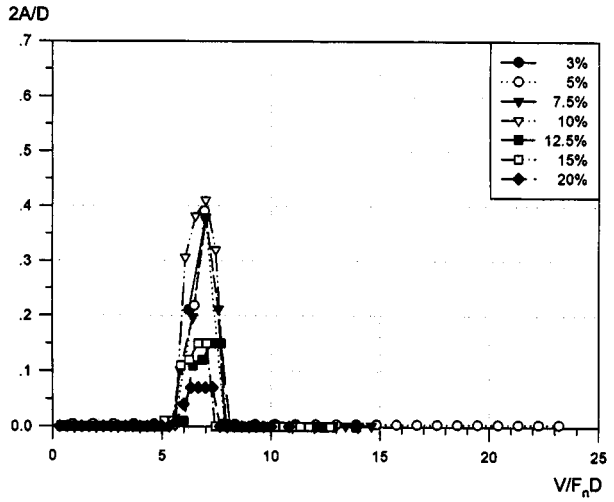

Fig. 16 The aerodynamic behaviors for the square model with corner cut (α=20°)

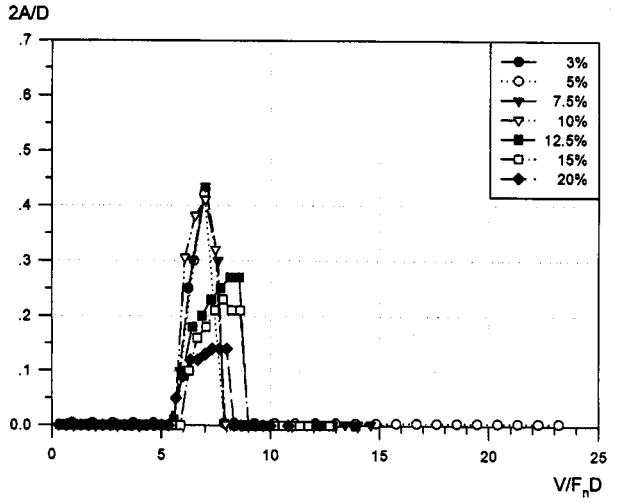

Fig. 17 The aerodynamic behaviors for the square model with corner cut (α=25°)

occurs at the same onset velocity of the galloping with as large amplitudes as that of square model. However, it is noted that at α=15°, there is virtually no VIV observed unlike the case of square model. The aerodynamic characteristics of this model is generally similar to that of the square model except a few cases (Figs. 14~20).

4.2. Blockage effect for the galloping and vortex-induced vibration

Fig. 14 shows the galloping at α=0°. The onset reduced velocity of the galloping has almost same trends regardless of the blockage ratios like the result of square model. However, there are distinguished two trends in aerodynamic responses. In case of models with up to 10% S/C, after developing the initial response at $V_r \cong 7.5$, the response decreases somewhat slightly for

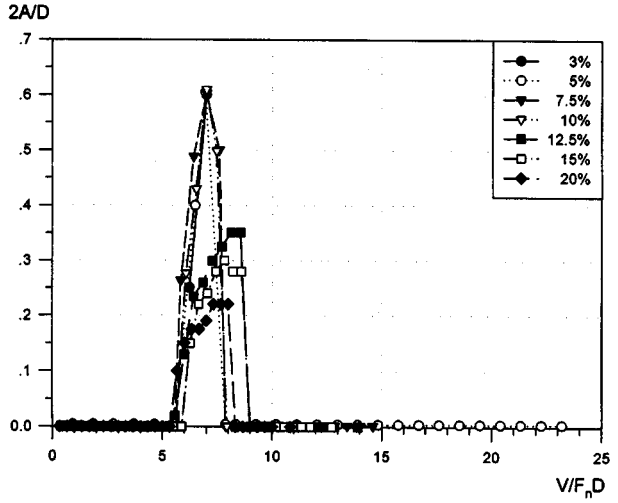

Fig. 18 The aerodynamic behaviors for the square model with corner cut (α=30°)

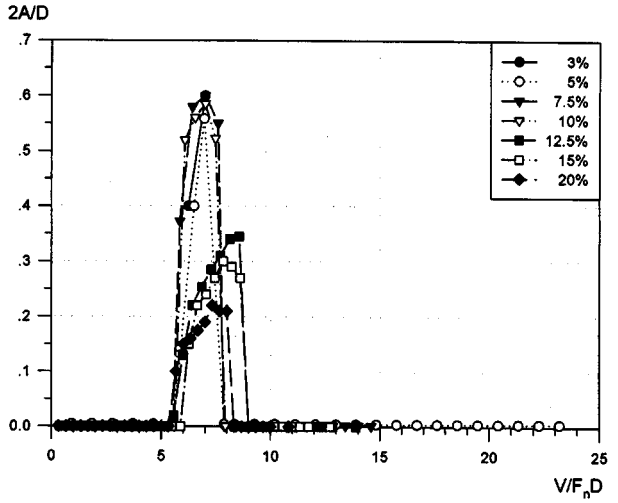

Fig. 19 The aerodynamic behaviors for the square model with corner cut (α=35°)

a short while, and then head up again at $V_r \cong 10.0$ which is considered as the final onset velocity for the galloping. In case of models with over 10% S/C, unlike the case of models with up to 10% S/C, the response develops continuously without decreasing after the initial development of the galloping. While the models with up to 10% S/C can describe the detailed behavior, the models with over 10% S/C can not describe such a detailed behavior. From these observations, it is tentatively concluded that models with up to 10% S/C produce almost same test results.

Test results of vortex-induced vibration is shown in Figs. 15~21. At α=15°, there is virtually no VIV observed (Fig. 15). Comparing with the test results of square model, it can be shown that the general trends of the results from two models, the square and square with corner cut, are in a good agreement and the onset and extinction reduced velocities ($V_r \cong 5.5$, 8.0 respectively),

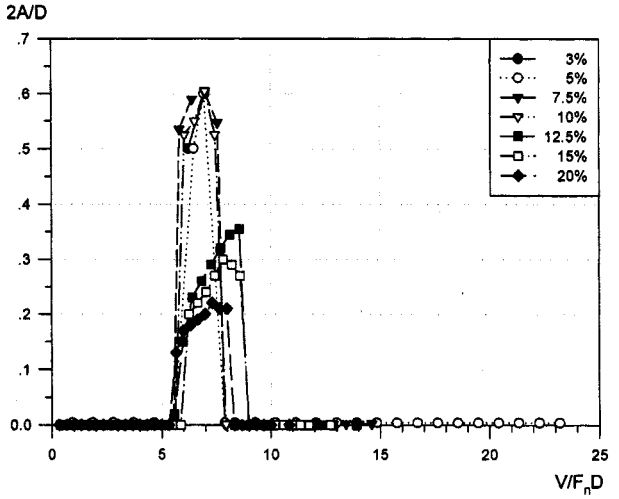

Fig. 20 The aerodynamic behaviors for the square model with corner cut (α=40°)

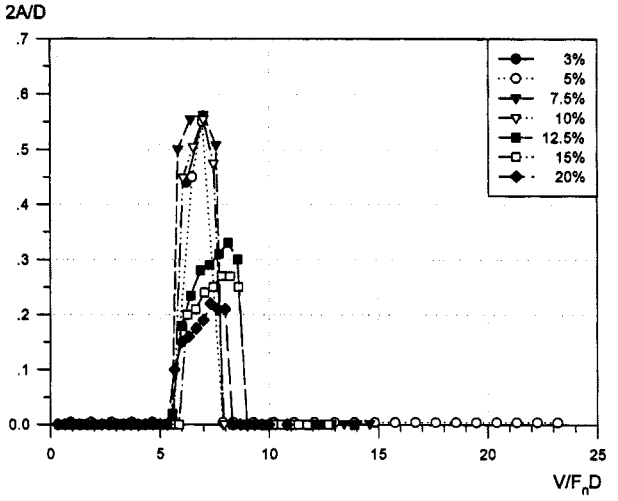

Fig. 21 The aerodynamic behaviors for the square model with corner cut (α=45°)

maximum response, and the velocity at which the maximum response occurs are nearly the same in case of models with up to 10% S/C. However, in case of models with over 10% S/C, these velocities are somewhat different like the results of square model. Similar trends are also observed for the case of models with over 10% S/C. Overall trends of results for the square model with corner cut are similar to those of square model.

5. Conclusions

This paper presents a parametric study on the wind tunnel blockage effect on the wind-induced dynamic characteristics of two test models, i.e., the square and the square with corner cut. A series of tests were carried out for the galloping phenomenon and vortex-induced

vibration with several different blockage ratios and different angles of attack. For models with up to 10% S/C as a group, the test results are almost identical, while for the models with over 10% S/C, the test results show some discrepancies. For the galloping phenomenon, the models produced almost the same onset reduced velocity and aerodynamic responses regardless of the blockage ratios of models. For the vortex-induced vibration, the models with up to 10% S/C produced virtually the same onset and extinction reduced velocities, the onset V_r of maximum response while the models with over 10% S/C produced large discrepancies in test results. From these tests, it has been concluded that the wind-induced dynamic characteristics of test models are in good agreements in case of models with up to 10% blockage ratios and the models with up to 10% blockage ratios can be treated as the same group which behaves similarly. Therefore, when the increased blockage ratio is required, the ratio may be increased up to 10% without any serious loss of accuracy of test results so that the manufacturing a more sophisticated and detailed test models will be possible.

References

ASCE Standard (1997), *Wind Tunnel Testing for Buildings and Other Structures*, June.

An Editorial Board of Bridge and Wind (1990), *The Bridge and Wind.*

Awbi, H.B. (1978), "Wind-tunnel-wall constraint on two-dimensional rectangular section prisms", *J. of Industrial Aerodynamics*, **3**.

Choi, C.K., Yu, W.J. and Kwon, D.K. (1998), "Comparison between the CFD and wind tunnel experiment for tall building with various corner shapes", *Proceedings of the Fifth International Conference on Tall Buildings*, Hong Kong, 632-637.

Choi, C.K. and Kwon, D.K. (1999), "An aerodynamic characteristics study on various section shapes of rectangular cylinder", *Journal of the Wind Engineering Institute of Korea.*

Cowdrey, C.F. (1967), "The application of Maskell's theory of wind tunnel blockage to very large solid models", *NPL Aero R.*1247.

Honshu-Shikoku Bridge Authority (1980), The Specification for the Wind-Resistant Design Code of Honshu-Shikoku bridge.

Honshu-Shikoku Bridge Authority (1990), The Specification for the Wind-Resistant Design Code and Explanation.

Houghton, E.L. and Carruthers, N.B. (1976), *Wind Force on Buildings and Structures*, Edward Arnold.

Japanese Architectural Center (1994), *A Guide book for Structural Engineers on the Wind Tunnel Test of Architectural Structures.*

Laneville, A. and Trepanier, J.Y. (1986), "Blockage effects in smooth and turbulent flows : The case of 2-D rectangular cylinders", *J. of Wind Eng. And Industrial Aerodynamics*, **22**.

Liu, H. (1991), *Wind Engineering* : A Handbook for Structural Engineers, Prentice-Hall.

Maskell, E.C. (1963), "A theory of the blockage effects on bluff bodies and stalled wings in a closed wind tunnel", *R & M*, No. 3400, ARC.

Noda, M., Utsunomiya, H. and Nagao, F. (1993), "Basic study on blockage effects in turbulent boundary layer flows", *Third Asia-Pacific Symposium on Wind Eng.*, 905-910, December 13-15.

Sykes, D.M. (1973), "Blockage corrections for large bluff bodies in wind tunnels", *BHRA Fluid Eng.*

Takeda, T. and Kato, M. (1992), "Wind tunnel effects on drag coefficient and wind-induced vibration", *Journal of Wind Engineering and Industrial Aerodynamics*, **41-44**, 897-908.

(Communicated by Chang-Koon Choi)